

Electron beam velocity effects with kappa distribution function on kinetic Alfvén waves in dusty plasma

Amar Singh Patneshwar¹, G.Ahirwar²

¹ School of studies in physics, Vikram university, Ujjain (M.P.)-456010

Abstract : The effect of electron beam on dispersion relation, and growth rate, perpendicular wave and marginal instability of the kinetic Alfvén waves with kappa distribution function in a low β homogeneous plasma is discussed by investigating the trajectories of the charge particles. Particle aspect approach is adopted to investigate the trajectories of charged particles in the electromagnetic field of kinetic Alfvén wave in the presence of kappa distribution function. Kinetic Alfvén wave with kappa distribution function in the presence of beam effects are investigated. Expressions are found for dispersion relation, growth rate and growth length for dust particle of charge. The results are interpreted for the space plasma parameter appropriate to the auroral acceleration region of earth's magnetosphere. Kinetic effects of electrons and ions are included to study kinetic Alfvén wave because both are important in the transition region.

Index terms: kinetic Alfvén wave, Magneto-plasma, Auroral acceleration region, kappa distribution function, dusty plasma, beam effect.

Introduction :

Kinetic Alfvén waves play an important role in energy transport in driving field-aligned currents, particle acceleration and heating, inverted-V structures in magnetosphere-ionosphere coupling, solar flares and the solar wind¹⁻⁷. They are also useful in explaining the ultra-low frequency emissions in the earth's magnetosphere. Field-aligned currents play a dominant role in the study of magnetized plasmas of magnetosphere-ionosphere coupling. The kinetic Alfvén waves may be generated by the density inhomogeneity of the plasma sheet and propagate to the ionosphere. Over the last decade it has been established that auroral luminosity is due to the impact of an accelerated electron beam coming towards the ionosphere and at the same event the up flowing ion beam has also been observed towards the magnetotail⁵⁻⁶. In the recent past the kinetic Alfvén wave has been analyzed using particle aspect analysis in view of the auroral acceleration processes⁸.

They are perhaps of most importance in magnetospheric physics in the study of coupling between regions, where different dynamical conditions prevail but which are threaded by the same field⁹. It has been established that auroral luminosity is due to the impact of an accelerated electron beam coming towards the ionosphere and at the same event the up flowing ion beam has also been observed towards the magnetotail^{10,11}. In the recent past particle aspect analysis was used to explain the auroral particle acceleration in the terms of Alfvén waves and kinetic Alfvén waves propagating parallel to or obliquely with respect to the ambient magnetic field¹²⁻¹³. One of the most important aspects of Alfvén waves observed in the auroral region, and more recently in the high latitude magnetosphere¹⁴ is its ability to accelerate electrons to energies sufficient to cause visible aurora¹⁵. Developed the idea that Alfvén wave with perpendicular wavelength of the order of an ion acoustic gyro radius or less, carries a parallel electric field and can, thereby, accelerate electrons to form aurora¹⁶.

Ion beam commonly believed to be produced by acceleration through a field aligned potential drop which also accelerates electrons downwards producing "inverted V" electron distributions²⁹. The ion beam energy is closely related to the magnitude of the potential drop estimated from the enhancement of the electron loss cones. In order to examine up flowing ions only near the auroral acceleration region, data were used from only near perigee which was at an altitude of about 0.8 RE over the southern polar region^{18,19} have stated that the ion beam considered does not follow the kappa distribution, it is background plasma of the auroral acceleration region which may permit the kappa distribution due to converging magnetic field lines. The ion beam is supposed to follow the drifting kappa distribution function²⁰. The ion beam in the direction of the wave motion may damp these waves if the ion beam velocity is smaller than the phase velocity of the wave; however, the ion beam opposite to the wave motion may excite the waves, as reported in this paper²⁰.

Hasegawa (1976)²¹ first suggested that small-scale kinetic Alfvén waves possessed parallel electric fields and could be an efficient mechanism for accelerating particles on plasma sheet field lines. The kinetic Alfvén waves Hasegawa had spatial scales perpendicular to B such that $k_{\perp}\rho_s \ll 1$, where ρ_s is the ion acoustic gyro radius. This is the "kinetic" limit of kinetic Alfvén waves. Subsequent theoretical investigations²² focused on kinetic Alfvén waves in the electron inertial limit for establishing parallel electric fields capable of accelerating auroral electrons. Considerable experimental evidence has accumulated from the Viking, Freja and FAST spacecraft, as well as low altitude sounding rockets, that kinetic Alfvén waves in the inertial limit are an important feature of the altitude range between 1000 km and 2.5 RE^{23,24}. Have presented a model calculation of the properties of kinetic Alfvén waves along a magnetic flux tube in which the altitude range encompasses both regimes.²⁶ Examined the importance of ions and electrons kinetic effects in the acceleration of electrons in small scale Alfvén waves above the auroral oval based on FAST satellite observations.²⁶

The transversely accelerated ions and their interaction with kinetic Alfvén waves in the auroral acceleration region have been recently reported by various workers.²⁷⁻³⁰ In the analysis of the FAST satellite data. The equilibrium dipolar magnetic field of the Earth is curved in a meridional plane and may introduce loss-cone effects in the particle distribution function.³¹⁻³⁴ In most of the theoretical work reported so far, the velocity distribution function has been assumed to be either ideally Maxwellian or bi-Maxwellian, ignoring the steep kappa function feature. Plasma in mirror-like devices and in the auroral region with curved and converging field lines,

depart considerably from a Max-wellian distribution and have a steep kappa distribution.^{33,35} In this paper we will discuss the effect of the kappa distribution function on the kinetic waves in the presence of ion beams and thermal anisotropy. The main objective of the present investigation is to examine the effect of ion beams on kinetic Alfvén waves at different kappa indices, in view of the observations in the auroral acceleration region. The present analysis is based on³⁶ theory of Landau damping, which was further extended.^{37-39,34} The method adopted, known as particle analysis, has been widely used in the analysis of electrostatic and electromagnetic instabilities.^{32,33,35,37,38} The relative importance of this approach over fluid and kinetic approach is also discussed.^{31,33,39} The main advantages of this approach is to consider the energy transfer between waves and particles, along with the discussion of waves dispersion and growth/damping rate of the waves. The method may be suitable to deal with the auroral electrodynamic where particle acceleration is also important along with waves emissions. The results obtained by this approach are the same as those derived using a kinetic approach⁴¹.

The kinetic Alfvén waves generated in the equatorial magneto- sphere travel towards the auroral ionosphere in the converging magnetic field; thus, it is assumed that the distribution may depart from ideally Max-wellian and allow for a kappa distribution function.^{34,35,38} In the past the mirror structure for the development of the quasi-static potential drop along auroral field lines has been adopted by various authors.⁴⁰ The various plasma instability processes may also lead to the kappa distribution.⁴¹ The mirror geometry is the justification of their choice and the experimental evidence is not known, to our knowledge. The ion beam considered does not follow the kappa distribution; it is the background plasma of the auroral acceleration which may permit the kappa distribution, due to converging magnetic field lines. The electron beam may generate the kinetic Alfvén waves, as mentioned in the Introduction. The ion beam in the direction of the wave motion may damp these waves, however, the ion beam opposite to the wave motion may excite the waves, as reported in this paper. In our present paper, we have considered the electrodynamic of the auroral ionospheric region by a kinetic Alfvén wave study.²⁸ predicted some observational evidences through satellite data. Ion conics may enhance the growth rate of kinetic Alfvén waves at the ionospheric region, which provides the potential of our theoretical model to study kinetic Alfvén wave characteristics in the auroral acceleration region.³⁴ The kinetic Alfvén turbulence plays an important role in the kappa relationship. It has been suggested that the kappa effects can enhance the anomalous resistivity for a given turbulence level. Since the steep kappa distribution in the presence of kinetic Alfvén waves and the ion beam enhances the growth rate, the anomalous resistivity and transport resulting from this instability are likely to play a crucial role in the auroral acceleration region. The converging magnetic field lines in the higher latitude auroral ionosphere may be considered suitable for the use of the generalized kappa distribution function. An upflowing ion beam, along with energetic particles may excite kinetic Alfvén waves. Both the ion and electrons are assumed to follow the kappa distribution function⁴¹.

Basic trajectory :

The kinetic Alfvén wave is assumed to start at t=0 when the resonant particles are undisturbed. The main interest lies in the behaviour of kinetic Alfvén waves, which satisfy the conditions.

$$V_{Tnd}, V_{Tni} \ll \frac{\omega}{K_{\perp}} \ll V_{Tne}; \quad \omega \ll \Omega_i; \quad \Omega_e, \Omega_d; \quad K_{\perp}^2 \rho_e^2 \ll K_{\perp}^2 \rho_i^2; \quad K_{\perp}^2 \rho_d^2 < 1 \tag{1}$$

Where V_{Tni} , V_{Tne} and V_{Tnd} are the mean velocities of ions, electrons and dust particles along the magnetic field, $\Omega_{i,e,d}$ are gyration cyclotron frequencies of the respective species. K_{\perp} and K_{\parallel} are the components of real wave vector k perpendicular and parallel to the magnetic field B_0 . Consider the two particles representation of electric field a kinetic Alfvén wave of the form (A K Dwivedi 2015)

$$\begin{aligned} E_{\perp} &= -\nabla_{\perp} \phi \text{ and } E_{\parallel} = -\nabla_{\parallel} \psi \\ \vec{E} &= \vec{E}_{\perp} + \vec{E}_{\parallel} \\ \phi &= \phi_1 \cos(k_{\perp}x + k_{\parallel}z - \omega t) \\ \psi &= \psi_1 \cos(k_{\perp}x + k_{\parallel}z - \omega t) \end{aligned} \tag{2}$$

where ϕ_1 and ψ_1 are assumed to be a slowly varying function of time t , and ω is the wave frequency which is assumed as real. $u_x(\vec{r}, t)$, $u_y(\vec{r}, t)$ and $u_z(\vec{r}, t)$ of the changed particles presence of KAW.

$$\begin{aligned} u_x(\vec{r}, t) &= -\frac{q}{m} \left[\phi_1 K_{\perp} - \frac{V_{\parallel} K_{\parallel} K_{\perp}}{\omega} (\phi_1 - \psi_1) \right] \sum_{-\infty}^{+\infty} J_n(\alpha) \sum_{-\infty}^{+\infty} J_l(\alpha) \left[\frac{\Lambda_n}{a_n^2} \cos \xi_{nl} - \frac{\delta}{2\Lambda_{n+1}} \cos(\xi_{nl} - \Lambda_{n+1}t) \right. \\ &\quad \left. - \frac{\delta}{2\Lambda_{n-1}} \cos(\xi_{nl} - \Lambda_{n-1}t) \right] \\ u_y(\vec{r}, t) &= -\frac{q}{m} \left[\phi_1 K_{\perp} - \frac{V_{\parallel} K_{\parallel} K_{\perp}}{\omega} (\phi_1 - \psi_1) \right] \sum_{-\infty}^{+\infty} J_n(\alpha) \sum_{-\infty}^{+\infty} J_l(\alpha) \left[\frac{\Omega}{a_n^2} \sin \xi_{nl} - \frac{\delta}{2\Lambda_{n+1}} \sin(\xi_{nl} - \Lambda_{n+1}t) \right. \\ &\quad \left. - \frac{\delta}{2\Lambda_{n-1}} \sin(\xi_{nl} - \Lambda_{n-1}t) \right] \\ u_z(\vec{r}, t) &= -\frac{q}{m} \left[\psi_1 k_{\parallel} - \frac{V_{\perp} K_{\parallel} K_{\perp}}{\omega} (\phi_1 - \psi_1) \frac{n}{\alpha} \right] \sum_{-\infty}^{+\infty} J_n(\alpha) \sum_{-\infty}^{+\infty} J_l(\alpha) \frac{1}{\Lambda_n} [\cos \xi_{nl} - \delta \cos(\xi_{nl} - \Lambda_n t)] \end{aligned} \tag{3}$$

Where $\delta=0$ for non-resonant particles and $\delta=1$ for resonant particle and $\Lambda_n = k_{\parallel} v_n - \omega + n\Omega$, $a_n^2 = \Lambda_n^2 - \Omega^2$

$$\alpha = \frac{K_{\perp} V_{\perp}}{\Omega},$$

$$\xi_{nl} = k_{\perp} x + k_{\parallel} z - \omega t + (l - n)(\theta - \Omega t) \quad (4)$$

θ is the initial phase of the velocity and $\Omega = qB_0/mc$, u_x and u_y are the perturbed and velocities in the x and y direction respectively. The slowly varying quantities ϕ_1 and ψ_1 are treated as a constant. Integration of eq. (3) gives the perturbed coordinates of particles x,y,z which in addition of trajectories of free gyration

Exhibits the true path of the particles. In the view of the approximations introduced in the beginning, the dominant contribution comes from the term $n=0$. J_s are Bessel's functions which arise from the different periodical variation of charged particles trajectories. The term represented by Bessel's functions show the reduction of the field intensities due to finite gyro radius effect. In order to find out the Density perturbation associated with the velocity perturbation, $\vec{u}(\vec{r}, t, \vec{v})$, we consider the equation for non-resonant particles

Distribution function:

The density perturbation associated with the velocity perturbation we consider the equation for non- resonant particles.

$$n_1(\vec{r}t) = F(\vec{v}) \sum_{-\infty}^{+\infty} J_n(\alpha) \sum_{-\infty}^{+\infty} J_1(\alpha) \frac{q}{m} \left[\left\{ \phi_1 \frac{v_{\parallel} k_{\parallel}}{\omega} (\phi_1 - \psi_1) \right\} \left\{ \frac{k_{\perp}^2}{a_n^2} + \frac{\Omega^2 v_d k_{\perp} m}{\Lambda_n a_n^2 T_{\perp}} \right\} + \frac{k_{\parallel}^2}{\Lambda_n} \left\{ \psi_1 - \frac{n v_{\perp} k_{\perp}}{\alpha \omega} (\phi_1 - \psi_1) \right\} \right] \cos \xi_{nl} \quad (5)$$

The resonant particles we have.

$$n_1(\vec{r}t) = F(\vec{v}) \sum_{-\infty}^{+\infty} J_n(\alpha) \sum_{-\infty}^{+\infty} J_1(\alpha) \frac{q}{m} \left[\left\{ \phi_1 \frac{v_{\parallel} k_{\parallel}}{\omega} (\phi_1 - \psi_1) \right\} \left\{ \frac{k_{\perp}^2}{a_n^2} + \frac{\Omega^2 v_d k_{\perp} m}{\Lambda_n a_n^2 T_{\perp}} \right\} \cos \xi_{nl} + \frac{1}{2\Omega \Lambda_{n+1}} \cos(\xi_{nl} - \Lambda_{n+1} t) \left(k_{\perp}^2 - \frac{\Omega v_d k_{\perp} m}{T_{\perp}} \right) \frac{v_d k_{\perp} m}{\Lambda_n T_{\perp}} \cos(\xi_{nl} - \Lambda_n t) - \frac{1}{2\Omega \Lambda_{n+1}} \cos(\xi_{nl} - \Lambda_{n-1} t) \left(k_{\perp}^2 + \frac{\Omega v_d k_{\perp} m}{T_{\perp}} \right) + \frac{k_{\parallel}^2}{\Lambda_n^2} \left\{ \psi_1 - \frac{n v_{\perp} k_{\perp}}{\alpha \omega} (\phi_1 \psi_1) \right\} \left\{ \cos \xi_{nl} + \Lambda_n t \sin(\xi_{nl} - \Lambda_n t) - \cos(\xi_{nl} - \Lambda_n t) \right\} \right] \quad (6)$$

Where $F(v)$ represent the kappa distribution function and V_d is the diamagnetic drift velocity which is defined by

$$V_d = \frac{T_{\perp}}{m\Omega} \varepsilon_N; \varepsilon_n = \frac{1}{N} \frac{dN}{dy} \text{ inhomogeneous}$$

To determine the dispersion relation and the growth rate, we use the by kappa distribution function with density perturbation .

Kappa distribution:

$$N(y, v) = N_0 \left[1 - \varepsilon \left(y + \frac{v_x}{\Omega} \right) \right] f_{\perp}(v_{\perp}) f_{\parallel}(v_{\parallel}) \quad (7)$$

Where

$$f_{\perp}(v_{\perp}) = \left[\frac{m v_{\perp}^2}{2K_B} \right] \frac{2k_{\perp}}{k_{\perp}^{-1}} \quad f_{\parallel}(v_{\parallel}) = \left[\frac{m v_{\parallel}^2}{2K_B} \right] \frac{2k_{\parallel}}{2k_{\parallel}^{-1}}$$

$$T_{\parallel c} = T_{\parallel} \left(\frac{2\kappa}{2\kappa-1} \right) \left[1 + i \frac{e_1 E_0 \bar{K}}{K^2 v_{T\parallel}^2 \left(\frac{2\kappa}{2\kappa-1} \right)} \right]$$

$$\text{and } K = (k_{\perp}^2 + k_{\parallel}^2)^{1/2}$$

And ε is a small parameter of the order of inverse of the density gradient scale length.

Dispersion relation:

To evaluated the dispersion relation, we calculate the integrated perturbed density for non-resonant particles as

$$n_{i,c,d} = \int_0^{\infty} 2\pi V_{\perp} dV_{\perp} \int_{-\infty}^{\infty} dV_{\parallel} n_i(r, t) \quad (8)$$

With

the help of eq.(5) and (7) use find the average densities for homogeneous plasma as

$$\bar{n}_i = \frac{\omega_{pi}^2}{4\pi e} \left[\frac{-K_{\perp}^2 \phi}{\Omega_i^2} + \frac{K_{\parallel}^2 \psi}{\omega_i^2} \right] \left(1 - \frac{1}{2} k_{\perp}^2 \rho_i^2 \right) \left(\frac{2k-1}{2k} \right) \quad (9)$$

$$n_e = \frac{\omega_{pe}^2}{4\pi e v_{T\parallel e}^2} \psi \quad (10)$$

$$\bar{n}_d = \frac{\omega_{pd}^2}{4\pi Z_d e} \left[\frac{-k_{\perp}^2 \phi}{\Omega_d^2} + \frac{k_{\parallel}^2 \psi}{\omega^2} \right] \left(1 - \frac{1}{2} k_{\perp}^2 \rho_d^2 \right) \left(\frac{2k-1}{2k} \right) \quad (11)$$

It

is observed that essential feature of the kinetic Alfvén wave is retained even in this ideal case. For maxwell's equation we use the quasi-neutrality condition,

$$\bar{n}_i = \bar{n}_e + Z_d \bar{n}_d$$

We get relation between ψ and ϕ as:

$$\phi = \frac{\Omega_d^2}{k_{\perp}^2} \left[\frac{\omega_{pc}^2}{\omega_{pd}^2 v_{T\parallel d}^2} - \frac{k_{\parallel}^2}{\omega^2} \left(1 + \frac{A_1 B_1}{A_2} \right) B_2^{-1} \psi \right] \quad (12)$$

Where

$$A_1 = 1 - \frac{1}{2} k_{\perp}^2 \rho_i^2 \left[\frac{2k_i-1}{2k_i} \right], \quad A_2 = 1 - \frac{1}{2} k_{\perp}^2 \rho_d^2 \left[\frac{2k-1}{2k} \right]$$

$$B_1 = \frac{N_0}{N_{d0}} \frac{m_d}{m_i} \frac{1}{z_d^2}, \quad B_2 = 1 - \frac{A_1 B_1}{A_2} \frac{\Omega_d^2}{\Omega_i^2}$$

Using perturbed ion, electron and dust particle densities n_i , n_e and n_d and Ampere's law in the parallel direction, we obtained the equation:

$$\frac{\partial}{\partial z} \nabla_{\perp}^2 (\phi - \psi) = \frac{4\pi}{c^2} \frac{\partial}{\partial t} J_z \quad (13)$$

where

$$J_z = c \int_0^{\lambda} ds \int_0^{\infty} 2\pi V_{\perp} dV_{\perp} \int_{-\infty}^{\infty} dV_{\parallel} \frac{m_j}{2} [(N + n_1)(V + u)^2 - NV^2]_j$$

J_z is the current density which is contributed by first-order perturbations of density and velocity. we obtain the dispersion relation for the kinetic Alfvén waves in homogeneous dusty plasma as:

$$\omega^4 \left(\frac{\omega_{pe}^2 B_2}{k_{\parallel}^4 \omega_{pd}^2 V_{Te}^4 V_A^2 A_2} \right) - \omega^2 \left\{ \frac{k_{\perp}^2 B_2}{k_{\parallel}^2 \Omega_d^2} \left(1 + \frac{\omega_{pd}^2 A_2}{c^2} \left(\frac{T_{\parallel cd}}{m_d} \right) \right) + \frac{\omega_{pi}^2 A_1}{c^2 k_{\parallel}^2 \Omega_d} \left(1 - \frac{\omega_{pi}^2}{\omega_{pd}^2 V_{Te}^2 \Omega_i^2 A_2} \frac{T_{\parallel ci}}{m_i} - \frac{k_{\perp}^2}{\Omega_i^2} \frac{T_{\parallel ci}}{m_i} \right) + \left(\frac{\omega_{pe}^2}{c^2 \Omega_d^2 V_{Te}^2 k_{\parallel}^2} \frac{T_{\parallel cd}}{m_d} \right) + \left(\frac{B_2}{k_{\parallel}^2 V_A^2} - \frac{\omega_{pe}^2}{k_{\parallel}^2 \omega_{pd}^2 V_{Te}^2 A_2} \right) \right\} - \frac{\omega_{pi}^2}{c^2 \Omega_i} \frac{T_{\parallel ci}}{m_i} \left(1 + \frac{A_1 B_1}{A_2} \right) - \frac{\omega_{pd}^2 A_2}{c^2 \Omega_d^2} \frac{T_{\parallel cd}}{m_d} - \frac{A_1 B_1}{A_2} + 1 = 0 \quad (14)$$

Where, $V_A^2 = \frac{c^2 \Omega_i^2}{\omega_{pd}^2}$ is the square of Alfvén's speed.

The oscillatory motion of non-resonant electrons carries the major part of energy. The wave energy density per unit wave length W_w is the sum of pure field energy and the changes in energy of the non-resonant particles $W_{i.e.d.}$. it is observed that the wave energy is contained in the form of the oscillatory motion of the non-resonant electrons.

Growth rate:

Using the law of conservation of energy, calculate the growth rate of drift kinetic Alfvén wave by

$$\frac{d}{dt} (W_w + W_r) = \quad (15)$$

With the help of we have found the growth rate of the drift kinetic Alfvén wave with dusty plasma as:

$$\frac{\gamma}{\omega} = \frac{\pi^{1/2} \omega_e}{k_{\parallel} V_{Te} \left[1 + \frac{\omega_{pi}^2 k_{\parallel}^2 T_{\parallel}}{\omega_e \omega_{pe}^2 m_e} (A_x + P_x) \right]} \frac{\Gamma(\kappa+1)}{\kappa^2 \times \Gamma(\kappa - \frac{1}{2})} \left(1 + \frac{(\omega_e)^2}{k_{\parallel}^2 v_{Te}^2} \right)^{-(\kappa+1)} \quad (16)$$

where $\omega_e = \omega - k_{\parallel} V_{de}$ electron beam velocity

Growth length:

$$\gamma = \frac{\Gamma(\kappa+1)}{\kappa^2 \times \Gamma(\kappa - \frac{1}{2})} \times \left[\frac{\sqrt{\pi} \times \sqrt{\omega_e}}{K_{\parallel} V_{Te} \left[1 + \frac{\omega_{pi}^2 V_{Te}^2}{\omega_e \omega_{pe}^2} (A_x + P_x) \right]} \cdot \left[1 + \frac{\omega_e}{K_{\parallel}^2 V_{Te}^2} \right] \right]^{-(\kappa+1)} \quad (17)$$

$$V_p = \left[\frac{B}{\omega_{pd}^2 V_{Te}^2 V_A^2 A_2} + \sqrt{B^2 + 4 \cdot \frac{\omega_{pe}^2 B_2}{\omega_{pd}^2 V_{Te}^2 V_A^2 A_2} \cdot C \cdot \frac{\omega_{pd}^2 V_{Te}^2 V_A^2 A_2}{\omega_{pe}^2 B_2}} \right]^{\frac{1}{2}} \quad (18)$$

$$L_g = \frac{\left[\frac{B}{\omega_{pd}^2 V_{Te}^2 V_A^2 A_2} + \sqrt{B^2 + 4 \cdot \frac{\omega_{pe}^2 B_2}{\omega_{pd}^2 V_{Te}^2 V_A^2 A_2} \cdot C \cdot \frac{\omega_{pd}^2 V_{Te}^2 V_A^2 A_2}{\omega_{pe}^2 B_2}} \right]^{\frac{1}{2}}}{\frac{\Gamma(\kappa+1)}{\kappa^2 \times \Gamma(\kappa - \frac{1}{2})} \times \left[\frac{\sqrt{\pi} \times \sqrt{\omega_e}}{K_{\parallel} V_{Te} \left[1 + \frac{\omega_{pi}^2 V_{Te}^2}{\omega_e \omega_{pe}^2} (A_x + P_x) \right]} \cdot \left[1 + \frac{\omega_e}{K_{\parallel}^2 V_{Te}^2} \right] \right]^{-(\kappa+1)}} \quad (19)$$

Where B and C are define as, and L_g is Growth length,

$$B = \frac{k_{\perp}^2 B_2}{k_{\parallel}^2 \Omega_d^2} \left(1 + \frac{\omega_{pd}^2 A_2}{c^2} \left(\frac{T_{\parallel cd}}{m_d} \right) \right) + \frac{\omega_{pi}^2 A_1}{c^2 k_{\parallel}^2 \Omega_d} \left(1 - \frac{\omega_{pi}^2}{\omega_{pd}^2 V_{Te}^2 \Omega_i^2 A_2} \frac{T_{\parallel ci}}{m_i} - \frac{k_{\perp}^2}{\Omega_i^2} \frac{T_{\parallel ci}}{m_i} \right) + \left(\frac{\omega_{pe}^2}{c^2 \Omega_d^2 V_{Te}^2 k_{\parallel}^2} \frac{T_{\parallel cd}}{m_d} \right) + \left(\frac{B_2}{k_{\parallel}^2 V_A^2} - \frac{\omega_{pe}^2}{k_{\parallel}^2 \omega_{pd}^2 V_{Te}^2 A_2} \right)$$

$$C = \frac{\omega_{pi}^2}{c^2 \Omega_i} \frac{T_{\parallel ci}}{m_i} \left(1 + \frac{A_1 B_1}{A_2} \right) - \frac{\omega_{pd}^2 A_2}{c^2 \Omega_d^2} \frac{T_{\parallel cd}}{m_d} - \frac{A_1 B_1}{A_2} + 1$$

Results and discussion:

$$\Omega_i = 412 \text{ s}^{-1}, \quad \Omega_d = 6.88 \times 10^{-10}, \quad m_d = 10^{-12} \text{ g}, \quad V_{Te} = 4 \times 10^6 \text{ ms}^{-1}, \quad \rho_i = 1.68 \times 10^4$$

$$N_d = 1 \times 10^3 \text{ cm}^{-3}, \quad Z_d = 5.5, \quad V_{de} = -1 \times 10^7,$$

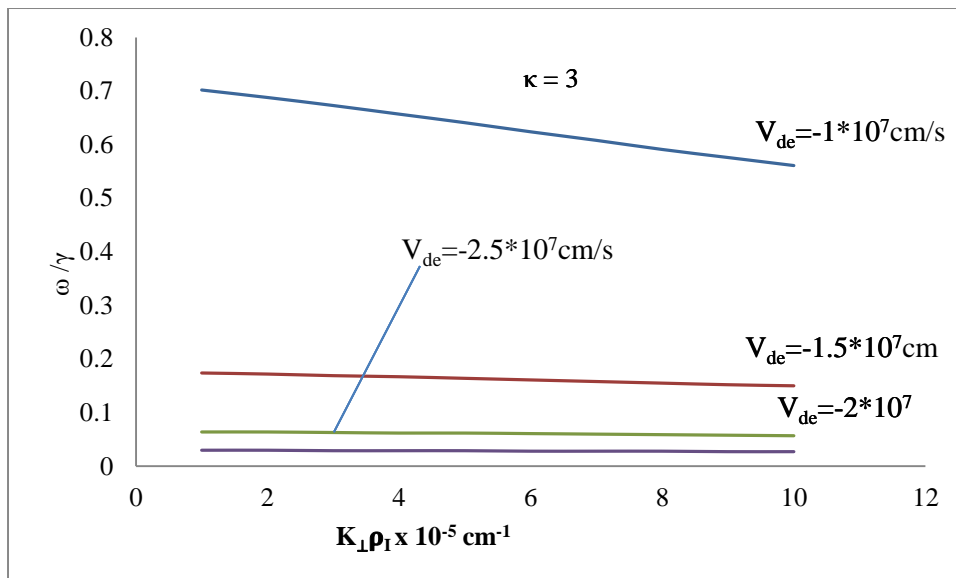


Fig.1 Variation of growth rate (γ/ω) versus perpendicular wave number ($K_{\perp} \rho_I$) for different value of electron beam velocities V_{de} . The variation of growth rate (γ/ω) with k_{\perp} at different values of electron beam velocities V_{de} at fixed values dust grain Z_d, N_d , and kappa κ . Here it is noticed that the effect of electron beam velocities is to reduced the growth rate at higher values of electron beam velocities with. Thus, the V_{de} controls the wave growth in the dusty magneto-plasma and transfers the energy to the particles by inverse Landau damping.

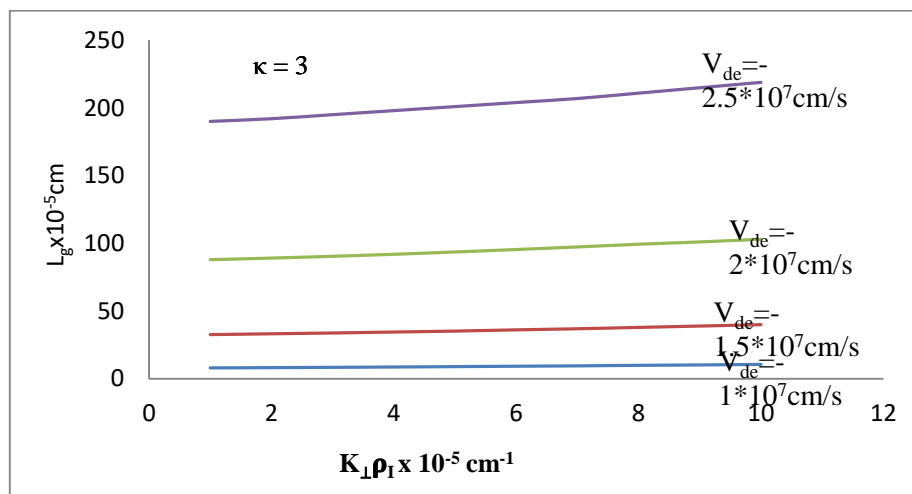


Fig. 2 The variation of growth length (γ_L) versus perpendicular wave vector ($K_{\perp} \rho_I$) cm^{-1} for different values of electron beam velocities V_{De} at kappa κ .

the relation between Growth length (L_g) versus perpendicular wave number k_{\perp} for different values of electron beam velocities V_{de} , at the fixed values of kappa κ and dust grain Z_d . It is observed that the electron beam velocities V_{de} , enhanced the frequency .it is clear that the growth length(L_g) increases with increase of applied electron beam velocities. the increase of growth length(L_g) with increasing $k_{\perp} \rho_i$.

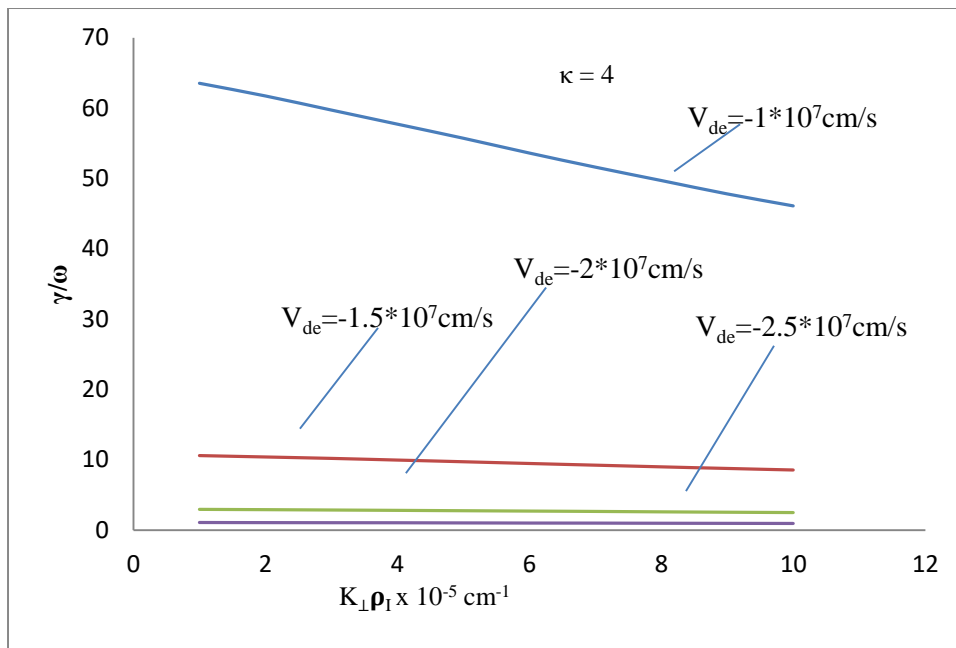


Fig.3 Variation of growth rate (γ/ω) with perpendicular wave number ($K_{\perp}\rho_I$) for different values of electron beam velocities at kappa (κ).

The variation of growth rate (γ/ω) with k_{\perp} at different values of electron beam velocities V_{de} at fixed values dust grain Z_d, N_d , and kappa $\kappa = 4$. Here it is noticed that the effect of electron beam velocities is to reduced the growth rate at higher values of electron beam velocities with. Thus, the V_{de} controls the wave growth in the dusty magneto-plasma and transfers the energy to the particles by inverse Landau damping.

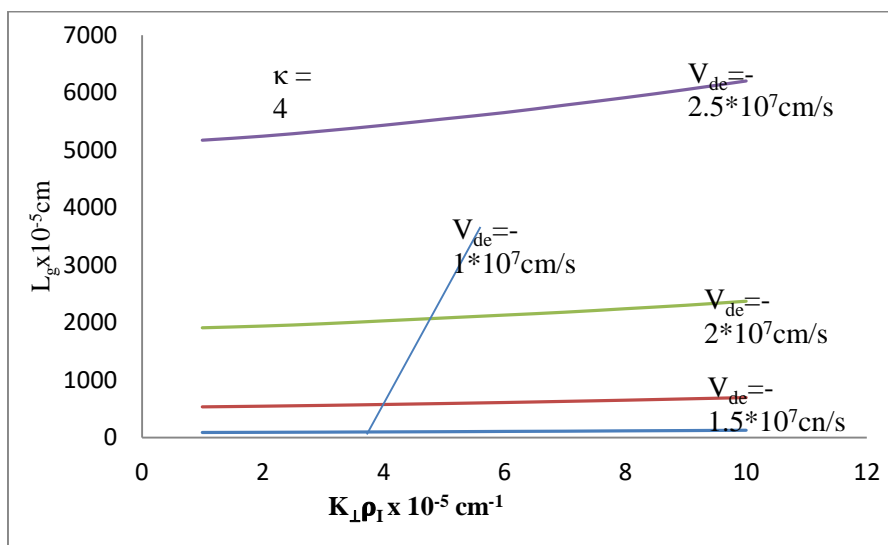


Fig. 4 The variation of growth length (γ_L) versus perpendicular wave vector ($K_{\perp}\rho_I$) cm^{-1} for different values of electron beam velocities V_{De} at kappa κ .

the relation between Growth length (L_g) versus perpendicular wave number k_{\perp} for different values of electron beam velocities V_{de} , at the fixed values of kappa $\kappa=4$ and dust grain Z_d . It is observed that the electron beam velocities V_{de} , enhanced the frequency .it is clear that the growth length(L_g) increases with increase of applied electron beam velocities. the increase of growth length(L_g) with increasing $k_{\perp}\rho_I$.

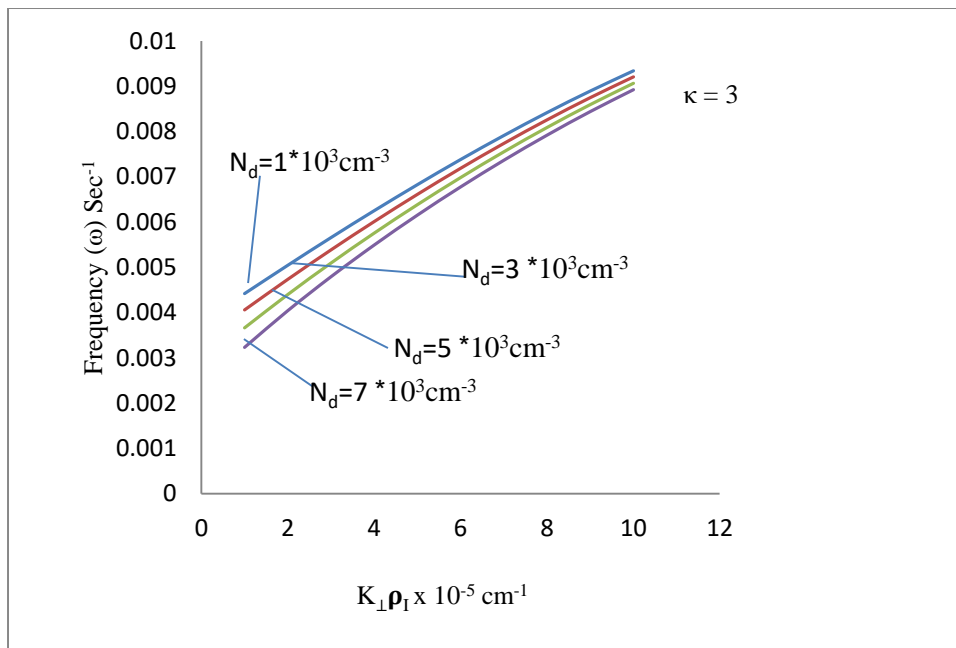


Fig.5 The variation of real frequency (ω) sec^{-1} versus perpendicular wave vector ($K_{\perp}\rho_I$) cm^{-1} for different values of N_d at kappa distribution function (κ).

shows the relation between wave frequency ω versus perpendicular wave number k_{\perp} for different values of N_d , at the fixed values of electron beam velocities V_{de} , dust grain Z_d and kappa (κ). It is observed that the N_d , enhanced the frequency. It is clear that the wave frequency ω increases with increase of applied N_d , the increase of ω with increasing k_{\perp} .

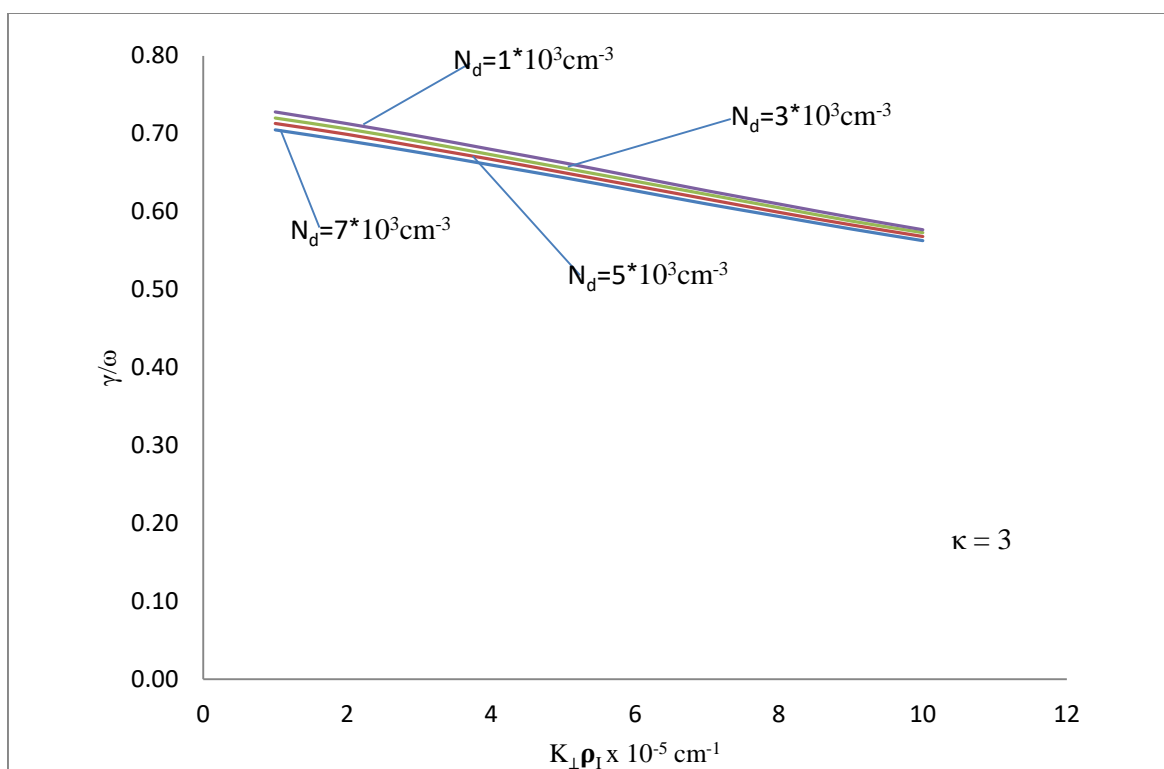


Fig. 6 The variation growth rate (γ/ω) versus perpendicular wave vector ($K_{\perp}\rho_I$) cm^{-1} for different values of N_d at kappa distribution function (κ).

The variation of growth rate (γ/ω) with k_{\perp} at different values of N_d at fixed values electron beam velocities V_{de} , dust grain Z_d and kappa κ . Here it is noticed that the effect of N_d is to reduced the growth rate at higher values of N_d with. Thus, the N_d controls the wave growth in the dusty magneto-plasma and transfers the energy to the particles by inverse Landau damping.

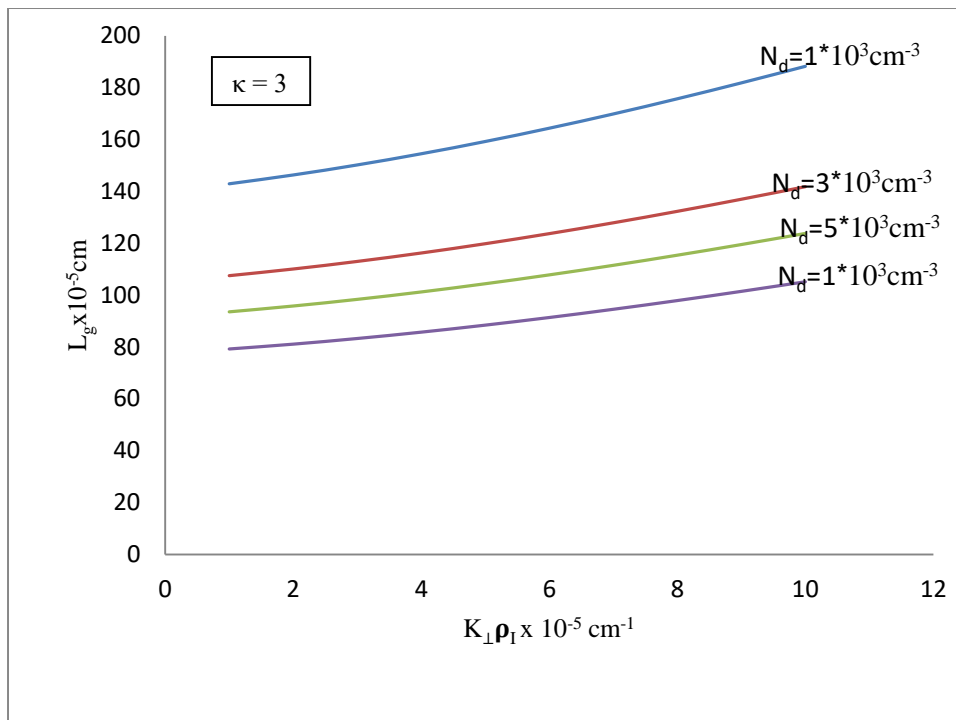


Fig.7 The variation of growth length (γ_L) versus perpendicular wave vector ($K_{\perp}\rho_i$) cm^{-1} for different values of N_d at kappa distribution function (κ).

the relation between Growth length (L_g) versus perpendicular wave number k_{\perp} for different values of N_d , at the fixed values of electron beam velocities V_{de} , dust grain Z_d and kappa ($\kappa=3$). It is observed that the N_d , enhanced the frequency .it is clear that the growth length(L_g) increases with increase of applied N_d . the increase of growth length(L_g) with decreasing $k_{\perp}\rho_i$.

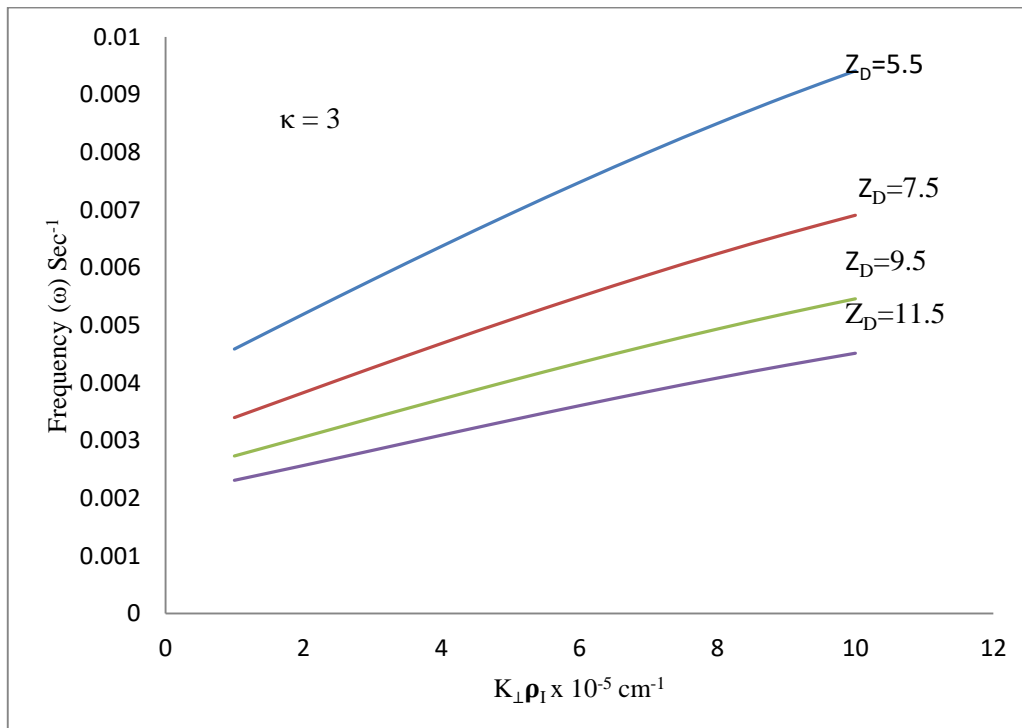


Fig. 8 The variation of real frequency (ω) sec^{-1} versus perpendicular wave vector ($K_{\perp}\rho_i$) cm^{-1} for different values of dust grain Z_d at kappa distribution function (κ).

shows the relation between wave frequency ω versus perpendicular wave number k_{\perp} for different values of dust grain Z_d , at the fixed values of electron beam effect V_{de} , $N_d=1*10^3\text{cm}^{-3}$ and kappa (κ). It is observed that the dust grain Z_d , enhanced the frequency. it is clear that the wave frequency ω increases with increase of applied dust grain Z_d . the increase of ω with increasing $k_{\perp}\rho_i$.

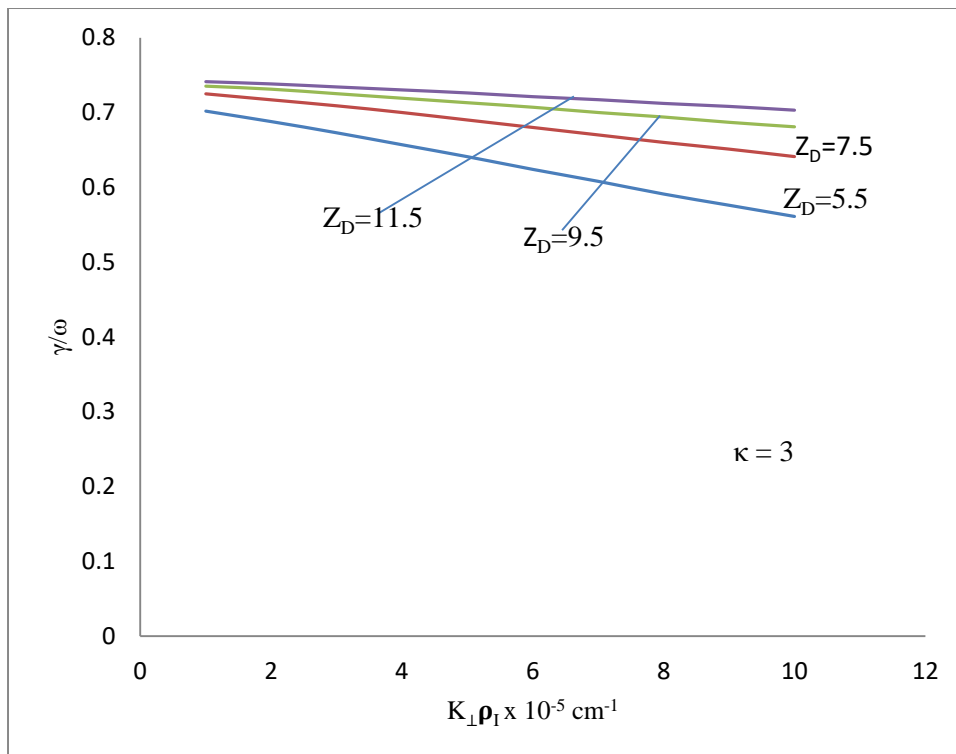


Fig. 9 The variation growth rate (γ/ω) versus perpendicular wave vector ($K_{\perp}\rho_I$) cm^{-1} for different values of dust grain Z_d at kappa distribution function (κ).

The variation of growth rate (γ/ω) with $k_{\perp}\rho_i$ at different values of dust grain Z_d at fixed values electron beam velocities V_{de} , N_d , and kappa κ . Here it is noticed that the effect of electric field is to reduced the growth rate at higher values of electric field with. Thus, dust grain Z_d controls the wave growth in the dusty magneto-plasma and transfers the energy to the particles by inverse Landau damping.

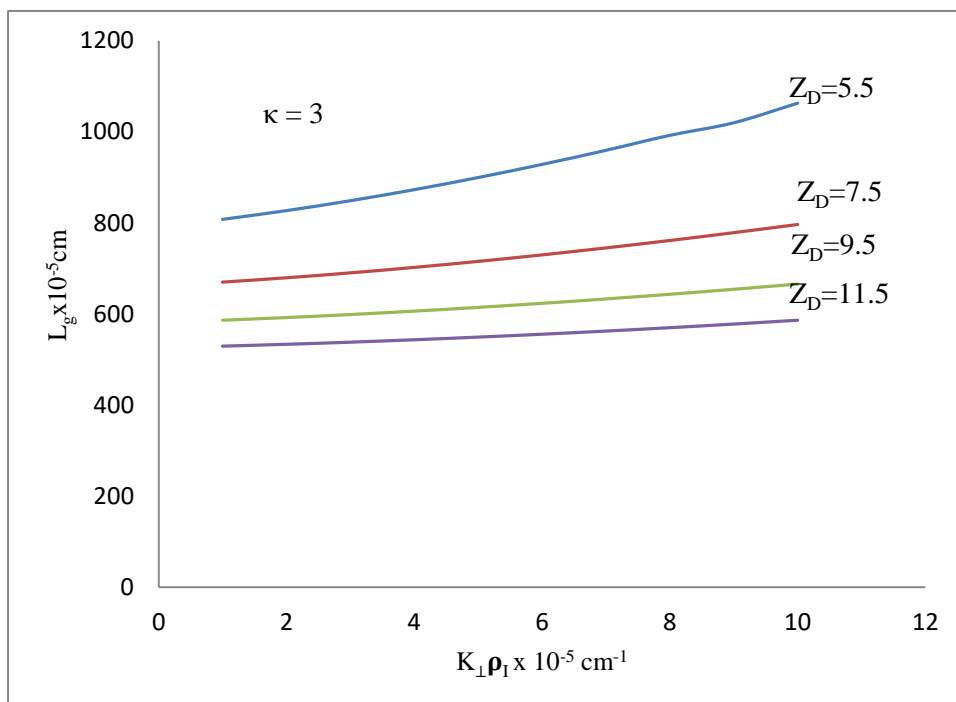


Fig. 10 The variation of growth length (γ_L) versus perpendicular wave vector ($K_{\perp}\rho_i$) cm^{-1} for different values of dust grain Z_d at kappa distribution function (κ).

the relation between Growth length (L_g) versus perpendicular wave number k_{\perp} for different values of dust grain Z_d , at the fixed values of electron beam velocities V_{de} , N_d , and kappa ($\kappa = 3$). It is observed that the dust grain Z_d , enhanced the frequency .it is clear that the growth length(L_g) increases with increase of applied dust grain Z_d . the increase of growth length(L_g) with decreasing $k_{\perp}\rho_i$.

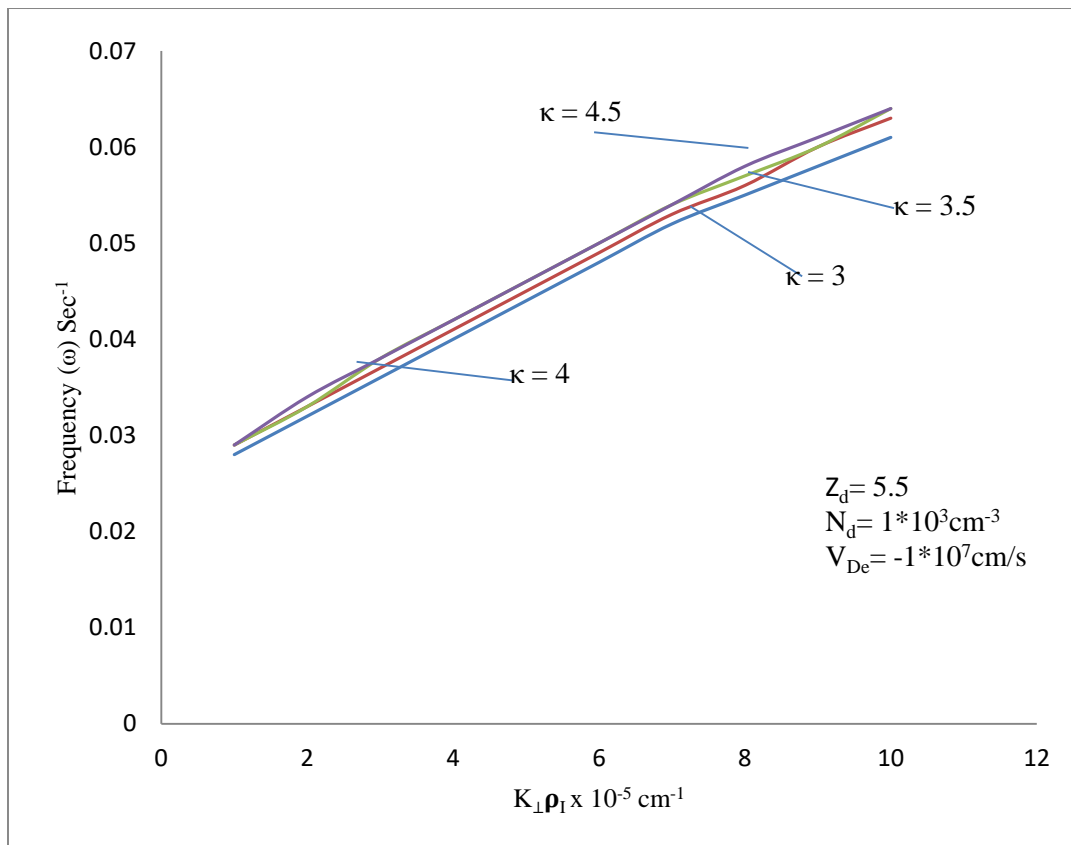


Fig. 11 The variation of frequency (ω) sec^{-1} versus perpendicular wave vector ($K_{\perp}\rho_1$) cm^{-1} for different values of kappa distribution function (κ) and fix value Z_d , N_d , and V_{de} .

shows the relation between wave frequency ω (rad/sec) versus perpendicular wave number k_{\perp} for different values of kappa distribution function κ , at the fixed values of dust grain Z_d and electron beam velocities V_{de} , and N_d . It is observed that the kappa distribution function κ , enhanced the frequency. It is clear that the wave frequency ω increases with increase of applied kappa function κ . The increase of ω with increasing k_{\perp} .

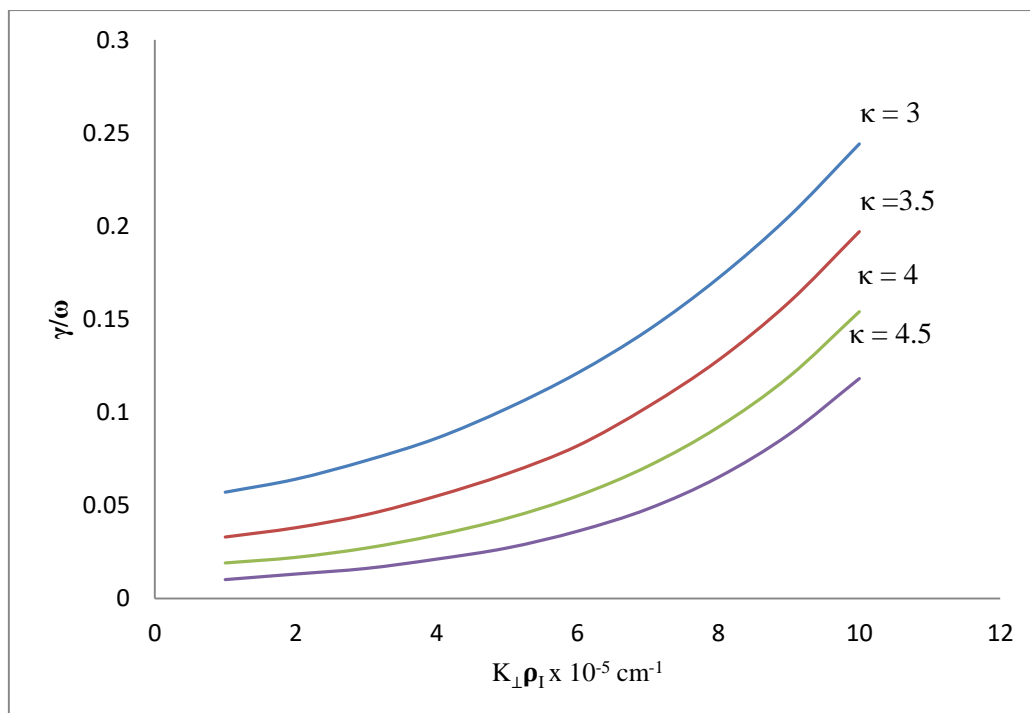


Fig. 12 The variation growth rate (γ/ω) versus perpendicular wave vector ($K_{\perp}\rho_1$) cm^{-1} for different values of kappa distribution function (κ) and fix value Z_d , N_d , and V_{de} .

The variation of growth rate (γ/ω) with k_{\perp} at different values of kappa distribution function κ at fixed values electron beam velocities V_{de} , N_d , and dust grain Z_d . Here it is noticed that the effect of kappa function is to reduced the growth rate at higher values of kappa κ with. The growth rate slows down as we increase the value of the kappa.

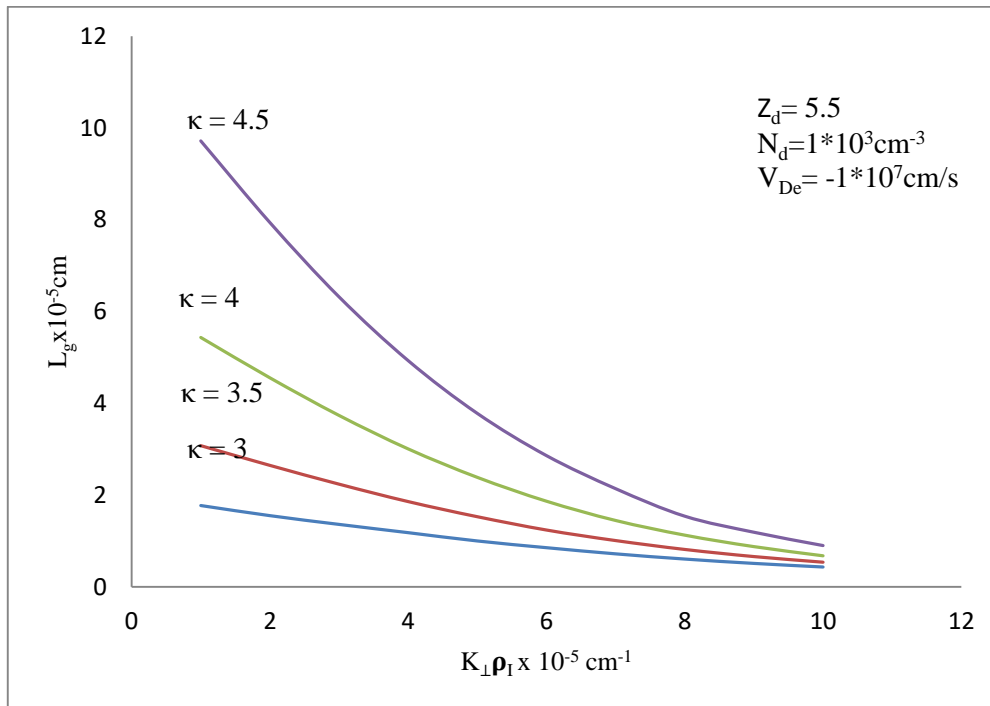


Fig. 13 The variation of growth length (γ_L) versus perpendicular wave vector ($K_{\perp}\rho_I$) cm^{-1} for different values of kappa distribution function (κ) and fix value Z_d , N_d , and V_{de} .

the relation between Growth length (L_g) versus perpendicular wave number k_{\perp} for different values of kappa function κ , at the fixed values of electron beam velocities V_{de} , N_d and dust grain Z_d . It is observed that the kappa function κ , enhanced the frequency. It is clear that the growth length (L_g) increases with increase of applied kappa function κ . The increase of growth length (L_g) with increasing $k_{\perp}\rho_I$.

Acknowledgements: We are thankful to Dr. G. Ahirwar for his valuable discussions. Financial assistance by Higher Education Department, M.P. is thankfully acknowledged.

References:

1. Hasegawa, A., 1977. Kinetic properties of Alfvén waves. Proc. Ind. Acad. Sci. 86A, 151.
2. Goertz, C.K., 1984. Kinetic Alfvén waves on auroral field lines. Planet. Space Sci. 32, 1387.
3. Goertz, C.K., Bosewell, R. W., 1979 Magnetosphere-ionosphere coupling. J. Geophys. Res. 84, 7293.
4. Marchenko, A V., Denton, RE., Hudson, M.K., 1996. A magnetospheric model of kinetic Alfvén waves with finite ion gyroradius. Phys. Plasmas 3, 3861.
5. Leonovich, A.S., Mazur, V.A, 1989. Resonance excitation of standing Alfvén waves in an axisymmetric magnetosphere (monochromatic oscillations). Planet Space Sci. 137, 1095.
6. Mozer, F.S, Wygant, JR, Boehm, M H, Cattell, C.A., Temerin, M., 1985. Large electric fields in the magnetosphere. Space Sci. Rev. 42, 313.
7. Klimushkin, D Y, 1997. Spatial structure of transversely small scale hydromagnetic waves in a plane finite- β model magnetosphere. Planet. Space Sci. 45, 269.
8. Huang, GL, Wang, R.Y, 1997. The growth of Alfvén waves in the resistive current driven instability J. Geophys. Res. 58, 433.
9. Southwood, D.J., Kivelson, M.G.: An approximate description of field- aligned currents in a planetary magnetic field. J. Geophys. Res. 96, 67 (1991).
10. Tiwari, M.S., Rostoker, G.: Field-aligned currents and auroral accelerations by non-linear MHD waves. Planet. Space Sci. 32, 1497 (1984).
11. Mozer, F.S., Wygant, J.R., Boehm, M.H., Ctell, C.A., Temerin, M.: Large electric fields in the magnetosphere. Space Sci. Rev. 42, 313 (1985).
12. Baronia, A., Tiwari, M.S.: Kinetic Alfvén wave in the presence of loss-cone distribution function in inhomogeneous magnetoplasma- particle aspect analysis. Planet. Space Sci. 47, 1111 (1999).
13. Dwivedi, A.K., Varma, P., Tiwari, M.S.: Kinetic Alfvén wave in the inhomogeneous magnetosphere and general distribution function. Planet. Space Sci. 49, 993 (2001).
14. Wygant i R 2000 Polar spacecraft based comparisons Poynting flux near and within the plasma sheet tail lobe boundary to UVI images: an energy source for the aurora J. Geophys. Res. 105 18675.
15. Hasegawa A 1976 Particle acceleration by MHD surface wave and formation of aurora J. Geophys. Res. 81 5083.
16. Schriver D 2003 Simulating an inhomogeneous plasma system: variable grids and boundary conditions Space Plasma Simulation (Lecture Notes in Physics vol. 615) ed J Büchner et al (New York: Springer-Verley).

17. Collin, H. L., Shelley, E. G., Ghielmetti, A. G., and Sherp, R. 29 D.: Observations of transverse and parallel acceleration of terrestrial ions at high altitudes in ion acceleration in the magnetosphere and ionosphere. Tom Chang. American Geophysical Union, Washington, 67, 1986.
18. Collin, H. L., Peterson, W. K., Lennartsson, O. W., and Drake, J. F.: The seasonal variation of Auroral Ion Beams, *Geophys. Res. Lett.*, 25 (21), 4071-4074, 1998.
19. Ahirwar, G., Varma, P., and Tiwari, M. S.: Beam effect on electromagnetic ion-cyclotron waves with general loss cone distribution function in an anisotropic plasma-particle aspect analysis, *Ann. Geophys.* 25, 557-568. doi:10.5194/angeo-25-557-2007, 2007.
20. GomberofT. L: Electrostatic waves in the Earth's magneto tail and in Comets and Electromagnetic instabilities in the magnetosphere and the solar wind, *IEEE Transactions on Plasma Sci.*, 20, 843- 866,1992.
21. Hasegawa, A. and Chen. L. (1975) Kinetic Process of Plasma Heating Due to Alfvén Wave Excitation. *Physical Review Letters.* 35, 370.
22. Goertz, C.K. and Boswell, R.W. (1979) Magnetosphere-Ionosphere Coupling. *Journal of Geophysical Research: Space Physics*, 84, 7239-7246.
23. Lysak. R.L. and Carlson. C.W. (1981) The Effect of Microscopic Turbulence Magnetosphere-Ionosphere Coupling. *Geophysical Research Letters*, 8, 269-272.
24. Lysak, R.L. and Lotko, W. (1996) On the Kinetic Dispersion Relation for Shear Alfvén Waves. *Journal of Geophysical Research: Space Physics*, 101, 5085-5094.
25. Chaston, C.C., Bonnell, J., Carlson, C.W., McFadden J.P., Ergun, R.E. and Strangeway, R.J. (2003) Kinetic Effects in the Acceleration of Electrons by Small Scale Alfvén Waves: A FAST Case Study. *Geophysical Research Letters*, 30, 1289.
26. Chaston, C.C., Carlson, C.W., Ergun, R.E., McFadden, J.P. and Strangeway, R.J. (2003) Properties of Small-Scale Alfvén Waves and Accelerated Electrons from FAST. *Journal of Geophysical Research: Space Physics*, 108, 8003.
27. Lund, E. J. Mobius, E., Klumpar, D. M., Kistler, L. M. Popecki. M. A., Klecker, B., Ergun. R. E., McFadden, J.P. Carlson, C. W., and Strangeway, R J: Occurrence distribution of preferentially heating events in the Aurora, *Adv. Space Res.*, 23, 1721-1724, 1999a.
28. Lund, E. J., Mobius, E., Carlson, C. W. Ergun. R. E., Kistler, L. M., Klecker, B., Klumpar. D. M., McFadden. J. P., Popecki. M. A., Strangeway, R. J., and Tung, Y. K.: Transverse ion acceleration mechanism in the aurora at solar minimum: occurrence distributions, *J. Atmos. Solar Terres. Phys.*, 62, 467-475, 2000.
29. Lund. E J. Mobius, E., Lynch KA Klumpar D M. Peterson. W K. Ergun. R E., and Carlson. C W On the Mass Dependence of Transverse Ion Acceleration by Broad Band Extremely Low Frequency Waves, *Phys. Chem. Earth* 26. 161-163. 2001.
30. Chaston. C. C. Carlson. C. W. Ergun, R. E., and McFadden, J. P FAST observations of inertial Alfvén waves in the dayside aurora. *Geophys. Res Lett.* 26. 647-650, 2002.
31. Varma, P and Tiwari. M. S.. Ion and electron beam effects on drift wave instability with different distribution function Particle aspect analysis. *Phys. Scr.* 45, 275-279, 1992.
32. Tiwari M. S and Varma P Drift instability in the presence of parallel electric field and an inhomogeneous magnetic field - Particle aspect analysis *J Plasma Phys.* 46, 49-62, 1991.
33. Tiwari M. S. and Varma. P Drift wave instability with loss cone distribution function particle aspect analysis, *Planet. Space Sci.* 41. 199 207: 1993.
34. Ahirwar, G Varma. P., and Tiwari, M. S.: Electromagnetic ion- cyclotron instability in the presence of parallel electric field with general distribution function Particle aspect analysis, *Ann. Geo- phys.* 24. 1919 1930 2006.
35. Duan S. P Li, Z Y, and Liu, Z. X.: Kinetic Alfvén wave driven by the density inhomogeneity in the presence of loss-cone distribution function Particle aspect analysis. *Planet. Space Sci.*, 53, 1167 1173. 2005.
36. Dawson J. On Landau Damping, *Phys. Fluids.* 4, 869-874 1961.
37. Dwivedi, A. K. Varma, P, and Tiwari, M. S.: Ion and electron beam effects on kinetic Alfvén wave in an inhomogeneous magnetosphere, *Planet Space Sci.*, 50, 93-99, 2002.
38. Mishra, R. and Tiwari, M. S. Effect of parallel electric field on electrostatic ion cyclotron instability in anisotropic plasma in the presence of ion beam and general distribution function, *Planet. Space Sci.*, 52, 188-199, 2006.
39. Varma, P and Tiwari. M. S: Drift wave in the presence of AC electric field with different distribution function particle aspect analysis. *Indian Journal of Pure Appl. Phys.*, 31, 616-623, 1993.
40. Schriver, D., Ashour-Abdalla, M. Strangeway, R.J. Richard. R L Klezting. C., Dotan, Y, and Wygant J FAST/Polar conjunction study of field aligned auroral acceleration and corresponding magneto-tail drivers, *J. Geophys Res.* 108(A9). 8020, 2003.
41. Horne, R. B. and Thorne. R. M.: Electron pitch angle diffusion by electrostatic electron cyclotron waves: the origin of pancake distributions, *J. Geophys. Res.*, 105, 5391-5402, 2000.